

Improving the accuracy of musculotendon models for the simulation of active lengthening

Matthew Millard^{A,B,C}, Fabian Kempter^B, Norman Stutzig^A, Tobias Siebert^{A,C}, and Jörg Fehr^{B,C}

Abstract Vehicle accidents can cause neck injuries which are costly for individuals and society. Safety systems could be designed to reduce the risk of neck injury if it were possible to accurately simulate the tissue-level injuries that later lead to chronic pain. During a crash, reflexes cause the muscles of the neck to be actively lengthened. Although the muscles of the neck are often only mildly injured, the forces developed by the neck's musculature affect the tissues that are more severely injured. In this work, we compare the forces developed by LS-DYNA's MAT_156 model and a newly proposed VEXAT model during active lengthening. The results show that Hill-type muscle models underestimate forces developed during active lengthening, while the VEXAT model can more accurately reproduce experimental results.

Keywords human body model, finite element, muscle model, neck injury, active lengthening

I. INTRODUCTION

Vehicle accidents often cause neck injuries [1] [2] that are costly to treat [3] and are difficult to predict using computer simulation [4] [5]. There is clinical evidence that people who suffer from chronic pain as a result of neck injury have sustained injuries to the facet joint capsules, the ligaments of the neck, intervertebral disks, and cervical vertebrae [6]. The musculature of the neck is important to accurately simulate because the tension developed by the muscles directly affects the stresses and strains of the tissues that are injured.

Experimental measurements of the kinematics and muscle activity during whiplash show that many of the neck's muscles are actively lengthened throughout a crash [7] [8]. When an active muscle is forcibly lengthened, it can develop tensions that greatly exceed the maximum isometric force (f_o^M) of the muscle [9] [10] right up until the muscle is injured [11] and ruptures at its failure force (f_F^M , $3.41 \pm 0.33 f_o^M$). Most of this tension is developed, particularly at long lengths [12] [13], by the semi-active titin filament [14] [15]. Hill-type muscle models [16] [17] are often used to simulate the musculotendon forces acting on human body models (HBMs) in FE simulations [18] [19] [20]. Hill-type muscle models lack a titin element since the formulation was developed decades [21] [22] [23] prior to the discovery of titin [14] [15]².

In this work, we simulate two active-lengthening experiments [9] [24] and compare the accuracy of the force response of LS-DYNA's MAT_156 [18] to our LS-DYNA implementation of VEXAT muscle model [25]. The VEXAT model [25] extends prior work that includes titin [26] [27] [28] by adding additional mechanical detail relevant to injury prediction — such as a viscoelastic cross-bridge and tendon — using only a few states beyond that of a conventional Hill-type model. First, we simulate the in-situ experiments of Herzog and Leonard [9] to directly compare the response of both models to the response of biological muscle. Next, we simulate a more aggressive active lengthening that takes each model through the various force thresholds of muscular injury [11]: mild injury ($2.39 f_o^M$ or $70\% f_F^M$), major injury ($3.07 f_o^M$ or $90\% f_F^M$), and finally rupture ($3.41 f_o^M$). The results of the Herzog and Leonard [9] simulation will show how accurately these two models are able to simulate modest active lengthening in comparison to biological muscle, while the response to aggressive lengthening will illustrate what can be expected during a more extreme event such as a crash simulation.

¹ M.Millard (+49 711 685 51763, matthew.millard@inspo.uni-stuttgart.de) is a Postdoctoral Researcher, F.Kempter is a Research Associate and Doctoral Student, E.Pelissetti is a Masters student, N.Stutzig is a Privatdozent, T.Siebert is a Professor, and J.Fehr is a Professor. The authors work at the ^AInstitute for Sport and Movement Science, ^BInstitute of Engineering and Computational Mechanics, and the ^CStuttgart Center of Simulation Science at the University of Stuttgart, Stuttgart, Germany.

² Titin is known as connectin in Japan, where it was first discovered by Maruyama [14]

41 A muscle model is defined by the experiments that it can replicate and the mechanisms that it embodies. Hill-
 42 type muscle models are phenomenological models because the formulation makes direct use of experimentally
 43 measured relationships without modelling the underlying processes. The tension (f^M) developed by the
 44 contractile element (CE) of LS-DYNA's MAT_156 [18] (Fig. 1A) is given by the product of the activation state of the
 45 muscle (a , which ranges between 0-1), the active-force-length relation ($\mathbf{f}^L(\ell^M)$), and the force-velocity relation
 46 ($\mathbf{f}^V(v^M)$)

$$47 \quad f^M = f_o^M (a \mathbf{f}^L(\ell^M) \mathbf{f}^V(v^M) + \mathbf{f}^{PE}(\ell^M)) \quad (1)$$

49 all of which is added to the elastic force developed by the parallel element ($\mathbf{f}^{PE}(\ell^M)$) (Fig. 1B). By construction,
 50 the Hill model can reproduce Hill's iconic force-velocity curve [21] during active shortening (concentric
 51 contraction). In addition, the model can also reproduce the passive [29] and active [30] isometric force-length
 52 relations. The MAT_156 implementation is stateless because it lacks activation dynamics and does not include an
 53 elastic tendon [18]. While the FE model can be edited to add an elastic tendon segment in series with a MAT_156
 54 element, care must be taken to ensure that the tendon properties scale with the f_o^M of the corresponding CE [31].

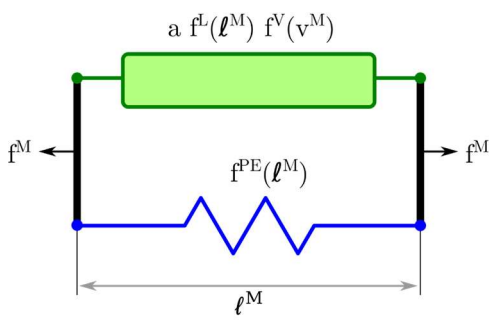
55 The VEXAT model [25](Fig. 1C) includes additional detail that is missing from Hill-type muscle models in general
 56 and the MAT_156 specifically (Fig. 1A). The VEXAT model derives its name from the lumped viscoelastic (VE) cross-
 57 bridge (X) and active-titin (AT) elements that it contains. The additional mechanical detail of the VEXAT model
 58 comes at the cost of five states to simulate activation dynamics (a), the position and velocity of the point of
 59 attachment of the lumped cross-bridge (XE) to actin (ℓ^S and v^S), the length of the CE (ℓ^M), and the position of
 60 the titin-actin bond (ℓ^1). The extra detail allows the active force developed by the CE (Fig. 1D),

$$61 \quad f^M = f_o^M (a \mathbf{f}^L(\ell^S + L^M)(k_o^X \ell^X + \beta_o^X v^X) + \mathbf{f}^2(\ell^2) + \mathbf{f}^{ECM}(\ell^{ECM}) + \beta^\varepsilon v^M - \mathbf{f}^{KE}(\ell^M) / \cos \alpha) \quad (2)$$

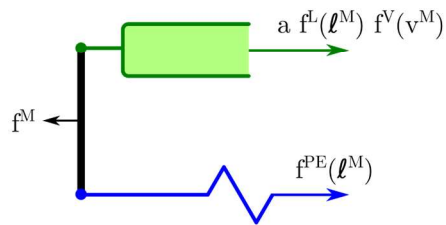
64 to be described in terms of the elastic ($k_o^X \ell^X$) and damping ($\beta_o^X v^X$) forces developed by the XE scaled by the
 65 proportion of attached cross-bridges ($a \mathbf{f}^L(\ell^S + L^M)$) of the model. The CE's passive forces come from the
 66 extracellular matrix ($\mathbf{f}^{ECM}(\ell^{ECM})$) and a mixture of active and passive forces from the distal segment of the titin
 67 model ($\mathbf{f}^2(\ell^2)$). The remaining two terms ensure that the model is stable during simulation ($\beta^\varepsilon v^M$) and cannot
 68 reach unrealistically short lengths ($\mathbf{f}^{KE}(\ell^M) / \cos \alpha$). The tension developed by the CE acts at a pennation angle
 69 α to the viscoelastic tendon (Fig. 1C and 1D). The pennation angle α is constrained to follow a specific length-
 70 angle relation in an effort to mimic the constant volume property of muscle [32]. As is typical [16], we assume
 71 that the muscle volume has a cross-section that is described as a constant height (h) parallelepiped where
 72 $\ell^M \sin \alpha = h$. While the VEXAT model may seem to only apply to a sarcomere (the smallest contractile element
 73 of a muscle - 2.73 μm long in humans), this model can be applied to whole muscle because the mechanical
 74 properties of sarcomeres scale with size: f_o^M scales with cross-sectional area [33], $\mathbf{f}^L(\ell^M)$ scales with length
 75 [34], the maximum shortening velocity scales with length [35], and titin's passive properties also scale with
 76 length [36] [37]. This model is both a mechanistic model and a phenomenological model in classification
 77 because it includes additional mechanical detail and yet still relies on phenomenological characteristics to drive
 78 the XE attachment point over time [25].

79 The active forces developed by titin, however, are not driven to follow any prescribed phenomena. To reduce
 80 the computational cost of simulating titin, the VEXAT model [25] treats titin as a two-segmented spring: the first
 81 spring spans a distance ℓ^1 from near the Z-line to the bond location within the titin element, while the second
 82 spring spans a distance ℓ^2 from the bond location to the myosin tip. Upon activation, damping forces are applied
 83 between the actin element and the point between the ℓ^1 and ℓ^2 segments. When titin is bound to actin, the ℓ^2
 84 element bares nearly all the strain, roughly doubling titin's stiffness compared to when the CE is passive. This
 85 modelling change leads to an important difference between the two models: the Hill model treats the active force
 86 response of muscle to lengthening as a velocity-dependent phenomenon, while the VEXAT model [25] treats this
 87 same process as both velocity and displacement-dependent phenomena.

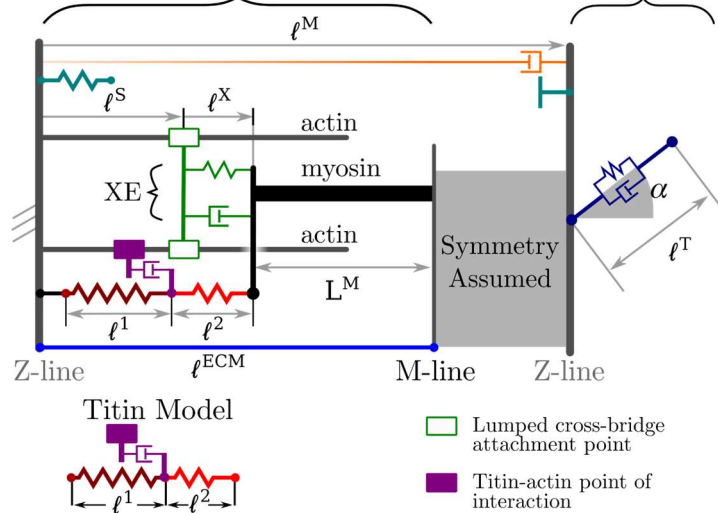
A) Hill-type muscle model MAT_156



B) MAT_156 model free-body diagram



C) The VEXAT muscle model of Millard et al. Half Sarcomere Model



D) The VEXAT model free-body diagram

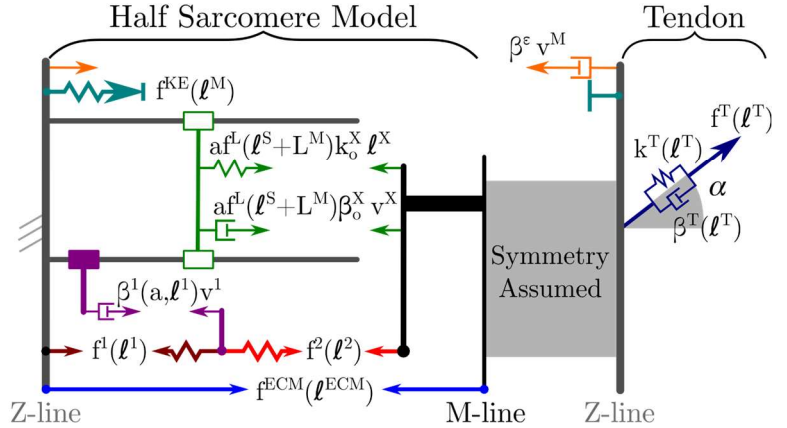


Fig. 1. LS-DYNA's Hill-type muscle model MAT 156 (A.) consists of an active element (green) in parallel with a passive element (blue) (B.). We have implemented the VEXAT (C.) model [25]³ as a material in LS-DYNA. The VEXAT model's active components include a lumped viscoelastic cross-bridge (green) and a semi-active titin element (D.). The passive elastic components of the VEXAT model include an elastic extracellular matrix ECM, a viscoelastic tendon (dark blue), and a small compressive element (blue-green) that prevents the contractile element (CE) from approaching unrealistically short lengths (D.). Upon activation, the damping forces (purple) slow the l^1 element, and the l^2 segment stretches (D.). Rigid components appear in black or dark grey, while the force-generating elements are illustrated in colour.

88 To fairly evaluate the two models, we have fitted the models to be as similar as possible to the cat soleus used
 89 in the experiments of Herzog and Leonard [9]. First, we have set the values of the optimal fibre length (l_o^M) and
 90 f_o^M of MAT_156 to be identical to the values produced by the VEXAT model when it is evaluated along the
 91 length of the tendon as shown in Table 1 (Appendix A). Since the VEXAT model includes a constant thickness
 92 pennation model [25], these properties differ slightly as the length and angle of the VEXAT's CE change with
 93 respect to the direction of the tendon. These differences are small because the fibres of a cat soleus are only
 94 pennated by 7° . Next, we have set the active-force-length and passive-force-length curves to fit the data of
 95 Herzog and Leonard [9] and to be identical when the VEXAT model is evaluated in the direction of the CE (Fig.
 96 2A). The passive force-length curves of the two models match if the CE is passive: as soon as the CE is active, the
 97 point between the l^1 and l^2 segments of the titin model viscously bond to actin and the stiffness of the titin
 98 filament and ECM together roughly doubles (Fig. 2A, magenta line). The curves that represent the passive force-
 99 length curves in MAT_156 and the ECM curves in VEXAT become linear when stretched sufficiently, as is typical

³ The images of the VEXAT model [25] have been used under the terms of the CC-BY license³ and have been modified from the original form. The images in this figure are also licensed under the terms of the CC-BY licence³. A copy of the licence can be found at <https://creativecommons.org/licenses/by/4.0/legalcode>

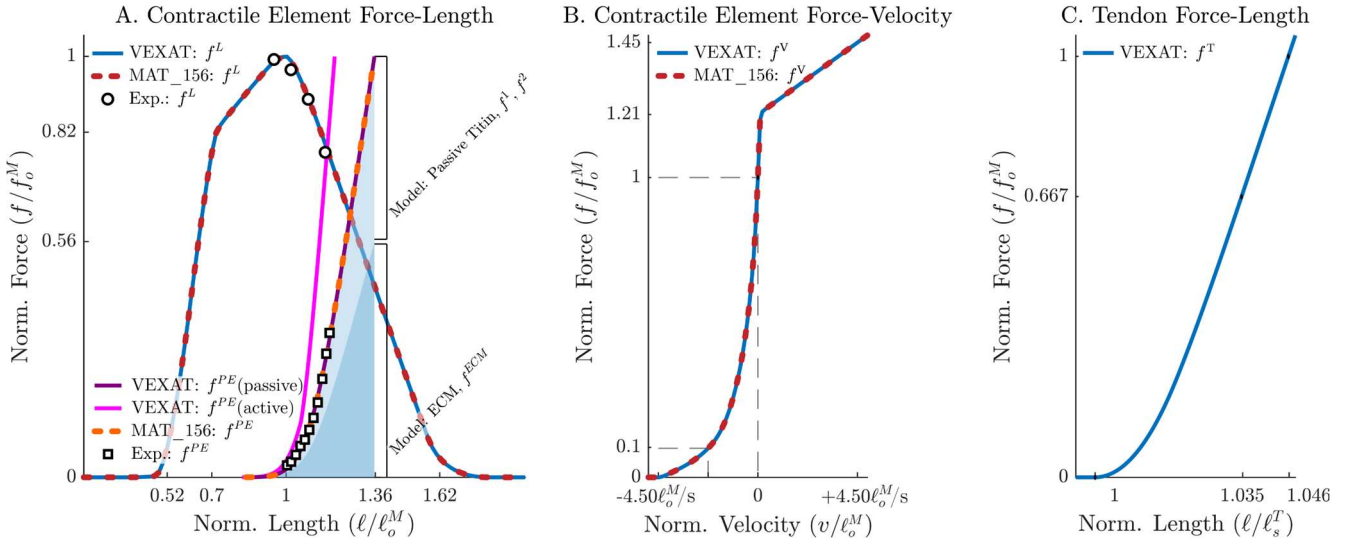


Fig. 2. The active and passive force-length curves (A) of the two models fit the data of Herzog and Leonard [9] and are identical when the VEXAT model is evaluated in the direction of the CE. The passive force-length curve of the VEXAT model is formed by a nearly equal contribution from the ECM and the titin element. When the CE is activated, the stiffness of titin increases and the force produced by the ECM and titin roughly doubles (magenta line). Both models have the same force-velocity curve (B) that fits the data of Scott et al. [38] during shortening and have been adjusted to fit the data of Herzog and Leonard [9] during lengthening. The VEXAT model includes a viscoelastic tendon (C), which has a nonlinear curve that fits the data from Scott et al. [39].

of skeletal muscle [40] [41]. Similarly, the force-length curves of titin's segments become linear at large strains, as indicated by the sarcomere-level experiments of Leonard et al. [12], even though this differs from a popular theoretical model (worm-like-chain model) of titin's force-length curve [42]. The bond location within the VEXAT's titin element has been chosen to fit the data of Herzog and Leonard [9]. Finally, Scott et al.'s measurements [38] have been used to fit the shortening side of the force-velocity curve, while the lengthening side of the curve has been fit to the data of Herzog and Leonard [9].

We first evaluate the models by comparing the peak forces developed during the active lengthening phase to the experimental data of Herzog and Leonard [9]. Next, we compare the root-mean-squared-error (RMSE) between each of the models and the experimental measurements during the active-lengthening phase of the experiment [9]. Although the experiment includes other phases, the active-lengthening phase has the largest forces and is thus the most relevant to the simulation of whiplash injury. In the second simulation, we evaluate the length change that each model must undergo to reach the threshold of minor injury since clinical evidence [6] suggests that minor injury to the neck muscles is commonly caused by whiplash.

III. RESULTS

The VEXAT model has an active lengthening force profile (Fig. 3A) that closely matches the data of Herzog and Leonard [9] both in peak value (35.7N vs 36.6N) and form (RMSE 0.8N) during the active lengthening phase between times 2.39s-3.39s (Fig. 3B) of the experiment. Although MAT_156 does develop enhanced forces during the active lengthening experiment, the peak forces are smaller than the experimental data (27.3 N vs 36.6 N), deviate from the experimental data (RMSE 4.7N), and are immediately reduced following the end of the ramp. In the normalised force-length space (Fig. 3C), it is clear that both the experimental data [9] and the VEXAT model develop active forces that grow in magnitude relative to the sum of the active and passive force-length curves (grey line). In contrast, the active force developed by the Hill model drops as the CE is lengthened further down the descending limb of the active force-length curve and will approach zero as the ℓ^M exceeds $1.62 \ell_o^M$ (Fig. 2A).

The tension developed by the VEXAT model increases faster than MAT_156 (Fig. 4A) if the ramp length is

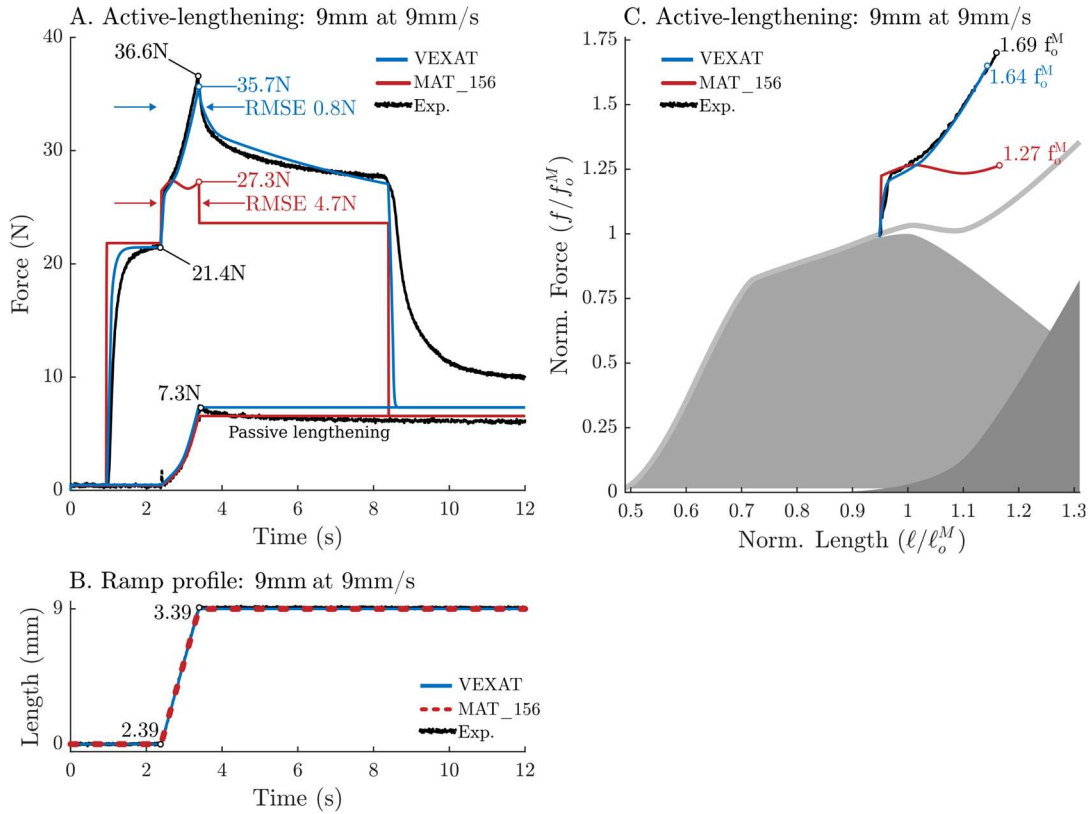


Fig. 3. During active lengthening, both the experimental data (Exp.) of Herzog and Leonard [9] and the VEXAT model develop a tension that increases as the muscle is lengthened (A). While the tension of the MAT_156 model does increase, it is short-lived and smaller in magnitude than the experimental data. The small differences that arise during the passive lengthening of the two models (A) are due to the elastic tendon of the VEXAT model and the pennation model, two components that MAT_156 lacks. The ramp-length change forced the models through a 9mm extension at a constant rate of 9mm/s (B). The tensions developed in the experiment and by the VEXAT model grow faster than the boundary formed by the active and passive-force length curves (C, grey line). The MAT_156 approaches the passive force-length curve as the contribution from the active-force-length curve decreases.

126 increased to 52 mm (Fig. 4B). As a result, the VEXAT model crosses the active minor injury force threshold of 2.39
 127 f_o^M [11] at a normalised length of 1.34 l_o^M , while the MAT_156 does not reach this threshold until the normalised
 128 length of 1.71 l_o^M (Fig. 4). The difference in normalised length between the two models at the threshold for minor
 129 injury (0.37 l_o^M) is similar at the thresholds for major injury (0.35 l_o^M), and rupture (0.35 l_o^M) (Fig. 4).

130 **IV. DISCUSSION**

131 Neck injuries sustained during vehicle accidents are common but perhaps could be prevented if it were
 132 possible to simulate the tissue-level injuries that lead to chronic pain. Great progress has been made in developing
 133 anatomically detailed male and female FE HBM models [4] [5], though Hill-type muscle models have been used
 134 to represent the musculature of the neck. Hill-type muscle models are not able to develop the large forces
 135 observed when biological muscle is actively lengthened. Since the muscles of the neck are known to be actively
 136 lengthened during whiplash [7] [8], we have compared in-situ experimental recordings of actively lengthened
 137 muscles to the simulated response of LS-DYNA's Hill-type muscle model (MAT_156) to the responses of the VEXAT
 138 model [25]. In contrast to MAT_156, the VEXAT model [25] includes a titin filament which produces enhanced
 139 forces during active lengthening [12] [13].
 140

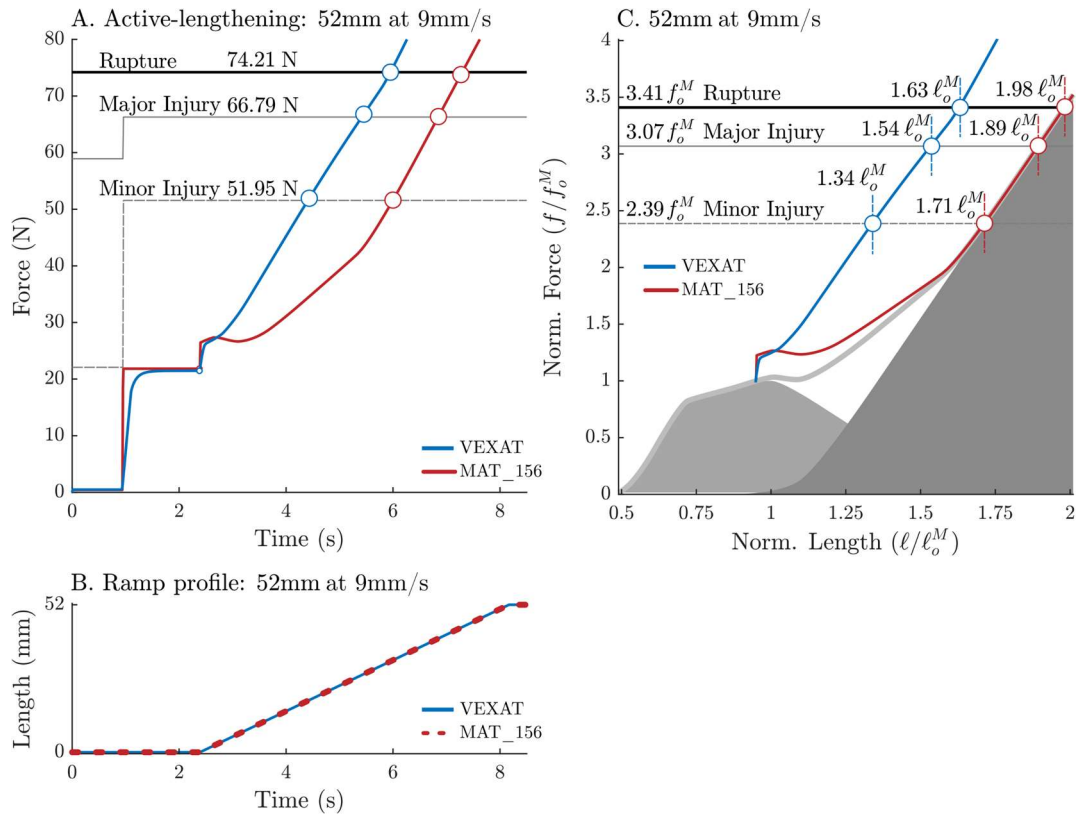


Fig. 4. Both the VEXAT and MAT_156 models develop forces that are large enough to pass through the active thresholds for minor injury, major injury, and rupture (A) when the ramp is extended from 9 mm to 52 mm (B). In a normalised force-length space (C), the VEXAT model passes through the thresholds for injury at shorter lengths than the MAT_156 model. This has implications for simulating whiplash: a muscle that is able to develop high forces at lower strains will reduce the amount of resulting head movement and will apply larger forces to the structures of the neck.

141 In our simulations of an in-situ active lengthening experiment, the VEXAT muscle produced force responses
 142 that more faithfully followed the experimental measurements than MAT_156 (Fig. 3). Unfortunately, we do not
 143 have experimental data that we can use to assess the accuracy of the aggressive active-lengthening injury
 144 simulation (Fig. 4), though our results highlight meaningful differences between the two models. While there are
 145 excellent lengthening injury datasets in the literature [24] [43], neither of these datasets contains the additional
 146 information that is required to fit the models to the specimen so that an accurate simulation of the experiment
 147 can be performed. Since titin has been shown to be capable of developing large forces in actively lengthened
 148 sarcomeres [12], we expect that the VEXAT model will produce more accurate results than a Hill-type model
 149 during the active lengthening that takes place during whiplash. While we hope to achieve improved accuracy
 150 during simulations of whiplash by including titin in the muscle model, other strategies have also been taken.

151 Biologically inspired controllers and Hill-type models have been used to improve the accuracy of simulated
 152 head and neck movement during whiplash. Models of the vestibulocollic and cervicocollic reflexes [44] [45], as
 153 well as stretch reflexes [46] [47], have improved the accuracy of head and neck models driven by Hill-type muscle
 154 models. More advanced Hill-type models than MAT_156 have also been developed to improve the response of
 155 the head and neck to sudden accelerations. The Hill-type model of Kleinbach et al. [19] [20] includes a more
 156 detailed activation dynamic and force-length model than is typical and was used to simulate the response of head
 157 movement to a sudden 1g acceleration [48]. Happee et al.'s [45] Hill-type model has been used to simulate the
 158 response of the head to vibration and to a sudden 15g acceleration [49]. While each of these works [44] [45] [46]
 159 [47] has shown improved results through the use of a biologically inspired controller, the results of these works
 160 are likely affected, to some degree, by the inaccurate force development of the underlying Hill-type model during
 161 active lengthening.

162 We have shown that a Hill-type muscle can underestimate the peak force developed by biological muscle by
 163 as much as 25% during an active lengthening experiment [9] with a modest 20% strain. Since mild muscle injury
 164 is often reported following whiplash [6], it is possible that Hill-type models are greatly underestimating the forces

165 applied by the neck muscles during simulations of whiplash. We plan to continue this work to see how these
166 models affect the kinematics, internal loads, and risk of injury during simulations of whiplash.

167 V. CONCLUSIONS

168 We found that the VEXAT model [25] can more accurately capture the force development of modestly actively
169 lengthened muscle than the MAT_156 Hill-type muscle model when compared to the experiments of Herzog and
170 Leonard [9]. The differences between the VEXAT and Hill-type muscle models are even more pronounced when
171 the models are actively lengthened to the point of mild injury: the VEXAT model reaches the force threshold for
172 mild injury at lengths $0.35 \ell_0^M$ shorter than in the Hill-type model. Taken together, it is likely that the Hill-type
173 muscle models used in simulations of car accidents have been underestimating the amount of force the
174 musculature of the neck applies to the cervical spine.

175 VI. ACKNOWLEDGEMENT

176 Funded by Deutsche Forschungsgemeinschaft (DFG, German Research Foundation) under Germany's
177 Excellence Strategy - EXC 2075 – 390740016. We acknowledge the support of the Stuttgart Center for Simulation
178 Science (SimTech).
179

180 VII. REFERENCES

- 181
- [1] C. S. B. Galasko, P. M. Murray, M. Pitcher, H. Chambers, S. Mansfield, M. Madden, C. Jordon, A. Kinsella and M. Hodson, "Neck sprains after road traffic accidents: a modern epidemic," *Injury*, vol. 24, p. 155–157, 1993.
 - [2] M. Richter, D. Otte, T. Pohlemann, C. Krettek and M. Blauth, "Whiplash-type neck distortion in restrained car drivers: frequency, causes and long-term results," *European Spine Journal*, vol. 9, p. 109–117, 2000.
 - [3] I. Carlsson, M. Hedin, J. A. Brorsson, S. Gårdestig, M. L. Lundgren, N. Rehnqvist, H. Danielsson and A. Lundius, "The whiplash commission final report," Klara Norra kyrkogata 33, 111 22 Stockholm, 2005.
 - [4] J. John, C. Klug, M. Kranjec, E. Svenning and J. Iraeus, "Hello, world! VIVA+: A human body model lineup to evaluate sex-differences in crash protection," *Frontiers in bioengineering and biotechnology*, vol. 10, 2022.
 - [5] D. Schwartz, B. Guleyupoglu, B. Koya, J. D. Stitzel and F. S. Gayzik, "Development of a computationally efficient full human body finite element model," *Traffic injury prevention*, vol. 16, p. S49–S56, 2015.
 - [6] G. P. Siegmund, B. A. Winkelstein, P. C. Ivancic, M. Y. Svensson and A. Vasavada, "The anatomy and biomechanics of acute and chronic whiplash injury," *Traffic injury prevention*, vol. 10, p. 101–112, 2009.
 - [7] J. R. Brault, G. P. Siegmund and J. B. Wheeler, "Cervical muscle response during whiplash: evidence of a lengthening muscle contraction," *Clinical biomechanics*, vol. 15, p. 426–435, 2000.
 - [8] A. N. Vasavada, J. R. Brault and G. P. Siegmund, "Musculotendon and fascicle strains in anterior and posterior neck muscles during whiplash injury," *Spine*, vol. 32, p. 756–765, 2007.
 - [9] W. Herzog and T. R. Leonard, "Force enhancement following stretching of skeletal muscle: a new mechanism," *The Journal of Experimental Biology*, vol. 205, p. 1275–1283, 2002.
 - [10] T. Siebert, K. Leichsenring, C. Rode, C. Wick, N. Stutzig, H. Schubert, R. Blickhan and M. Böl, "Three-dimensional muscle architecture and comprehensive dynamic properties of rabbit gastrocnemius, plantaris and soleus: input for simulation studies," *PLoS one*, vol. 10, p. e0130985, 2015.
 - [11] L. V. Nölle, A. Mishra, O. V. Martynenko and S. Schmitt, "Evaluation of muscle strain injury severity in active human body models," *Journal of the mechanical behavior of biomedical materials*, vol. 135, p. 105463, 2022.
 - [12] T. R. Leonard, V. Joumaa and W. Herzog, "An activatable molecular spring reduces muscle tearing during extreme stretching," *Journal of biomechanics*, vol. 43, p. 3063–3066, 2010.
 - [13] A. Tomalka, C. Rode, J. Schumacher and T. Siebert, "The active force–length relationship is invisible during extensive eccentric contractions in skinned skeletal muscle fibres," *Proceedings of the Royal Society B: Biological Sciences*, vol. 284, p. 20162497, 2017.
 - [14] K. Maruyama, "Connectin, an elastic protein from myofibrils," *The Journal of Biochemistry*, vol. 80, p. 405–407, 1976.
 - [15] K. Wang, J. McClure and A. N. N. Tu, "Titin: major myofibrillar components of striated muscle," *Proceedings of the National Academy of Sciences*, vol. 76, p. 3698–3702, 1979.
 - [16] F. E. Zajac, "Muscle and tendon: Properties, models, scaling, and application to biomechanics and motor control," *Critical Reviews in Biomedical Engineering*, vol. 17, p. 359–411, 1989.

- [17] T. Siebert and C. Rode, "6 - Computational modeling of muscle biomechanics," in *Computational Modelling of Biomechanics and Biotribology in the Musculoskeletal System*, Z. Jin, Ed., Woodhead Publishing, 2014, pp. 173-204.
- [18] B. Gladman, "LS-DYNA Keyword User's Manual: Volume II Material Models," 2016.
- [19] C. Kleinbach, O. Martynenko, J. Promies, D. F. B. Haeufle, J. Fehr and S. Schmitt, "Implementation and validation of the extended Hill-type muscle model with robust routing capabilities in LS-DYNA for active human body models," *Biomedical engineering online*, vol. 16, p. 1–28, 2017.
- [20] D. F. B. Haeufle, M. Günther, A. Bayer and S. Schmitt, "Hill-type muscle model with serial damping and eccentric force–velocity relation," *Journal of biomechanics*, vol. 47, p. 1531–1536, 2014.
- [21] A. V. Hill, "The heat of shortening and the dynamics constants of muscle," in *Proceedings of the Royal Society of London*, 1938.
- [22] D. R. Wilkie, "The mechanical properties of muscle," *British medical bulletin*, vol. 12, p. 177–182, 1956.
- [23] J. M. Ritchie and D. R. Wilkie, "The dynamics of muscular contraction," *The Journal of physiology*, vol. 143, p. 104, 1958.
- [24] C. T. Hasselman, T. M. Best, A. V. Seaber and W. E. Garrett JR, "A threshold and continuum of injury during active stretch of rabbit skeletal muscle," *The American Journal of Sports Medicine*, vol. 23, p. 65–73, 1995.
- [25] M. Millard, D. W. Franklin and W. Herzog, "A three filament mechanistic model of musculotendon force and impedance," *bioRxiv*, 2023.
- [26] C. Rode, T. Siebert and R. Blickhan, "Titin-induced force enhancement and force depression: a 'sticky-spring' mechanism in muscle contractions?," *Journal of theoretical biology*, vol. 259, p. 350–360, 2009.
- [27] G. Schappacher-Tilp, T. Leonard, G. Desch and W. Herzog, "A novel three-filament model of force generation in eccentric contraction of skeletal muscles," *PloS one*, vol. 10, p. e0117634, 2015.
- [28] K. Nishikawa and T. G. Huck, "Muscle as a tunable material: implications for achieving muscle-like function in robotic prosthetic devices," *Journal of Experimental Biology*, vol. 224, p. jeb225086, 2021.
- [29] A. M. Gordon, A. F. Huxley and F. J. Julian, "Tension development in highly stretched vertebrate muscle fibres," *The Journal of physiology*, vol. 184, p. 143–169, 1966.
- [30] A. M. Gordon, A. F. Huxley and F. J. Julian, "The variation in isometric tension with sarcomere length in vertebrate muscle fibres," *The Journal of Physiology*, vol. 184, pp. 170-192, 1966.
- [31] M. B. Bennett¹, R. F. Ker¹, N. J. Imery and R. M. Alexander¹, "Mechanical properties of various mammalian tendons," *Journal of Zoology*, vol. 209, pp. 537-548, 1986.
- [32] J. Swammerdam, "The Book of Nature II," *London: Seyffert*, p. 122–132, 1758.
- [33] C. N. Maganaris, V. Baltzopoulos, D. Ball and A. J. Sargeant, "In vivo specific tension of human skeletal muscle," *Journal of applied physiology*, vol. 90, p. 865–872, 2001.
- [34] T. M. Winters, M. Takahashi, R. L. Lieber and S. R. Ward, "Whole muscle length-tension relationships are accurately modeled as scaled sarcomeres in rabbit hindlimb muscles," *Journal of Biomechanics*, vol. 44, p. 109–115, 2011.
- [35] L. C. Rome, A. A. Sosnicki and D. O. Goble, "Maximum velocity of shortening of three fibre types from horse soleus muscle: implications for scaling with body size.," *The Journal of Physiology*, vol. 431, p. 173–185, 1990.
- [36] J. A. Herzog, T. R. Leonard, A. Jinha and W. Herzog, "Are titin properties reflected in single myofibrils?," *Journal of biomechanics*, vol. 45, p. 1893–1899, 2012.
- [37] L. G. Prado, I. Makarenko, C. Andresen, M. Krüger, C. A. Opitz and W. A. Linke, "Isoform diversity of giant proteins in relation to passive and active contractile properties of rabbit skeletal muscles," *The Journal of general physiology*, vol. 126, p. 461–480, 2005.
- [38] S. H. Scott, I. E. Brown and G. E. Loeb, "Mechanics of feline soleus: I. Effect of fascicle length and velocity on force output," *Journal of Muscle Research & Cell Motility*, vol. 17, p. 207–219, 1996.
- [39] S. H. Scott and G. E. Loeb, "Mechanical properties of aponeurosis and tendon of the cat soleus muscle during whole-muscle isometric contractions," *Journal of Morphology*, vol. 224, p. 73–86, 1995.
- [40] J.-S. Sun, Y.-H. Tsuang, T.-K. Liu, Y.-S. Hang and C.-K. Cheng, "Failure sites and peak tensile forces of the composite triceps surae muscle by passive extension in the rabbit," *Clinical Biomechanics*, vol. 9, p. 310–314, 1994.
- [41] T. Siebert, C. Rode, W. Herzog, O. Till and R. Blickhan, "Nonlinearities make a difference: comparison of two common Hill-type models with real muscle," *Biological cybernetics*, vol. 98, p. 133–143, 2008.
- [42] H. Granzier, M. Kellermayer, M. Helmes and K. Trombitás, "Titin elasticity and mechanism of passive force development in rat cardiac myocytes probed by thin-filament extraction," *Biophysical Journal*, vol. 73, p. 2043–2053, 1997.
- [43] T. J. Noonan, T. M. Best, A. V. Seaber and W. E. Garrett Jr, "Identification of a threshold for skeletal muscle injury," *The American journal of sports medicine*, vol. 22, p. 257–261, 1994.
- [44] M. A. Correia, S. D. McLachlin and D. S. Cronin, "Vestibulocollic and cervicocollic muscle reflexes in a finite element neck model during multidirectional impacts," *Annals of Biomedical Engineering*, vol. 49, p. 1645–1656, 2021.

- [45] R. Happee, E. de Bruijn, P. A. Forbes and F. C. T. van der Helm, "Dynamic head-neck stabilization and modulation with perturbation bandwidth investigated using a multisegment neuromuscular model," *Journal of biomechanics*, vol. 58, p. 203–211, 2017.
- [46] J. Östh, K. Brodin, S. Carlsson, J. Wismans and J. Davidsson, "The occupant response to autonomous braking: a modeling approach that accounts for active musculature," *Traffic injury prevention*, vol. 13, p. 265–277, 2012.
- [47] I. P. A. Putra, J. Iraeus, F. Sato, M. Y. Svensson, A. Linder and R. Thomson, "Optimization of female head–neck model with active reflexive cervical muscles in low severity rear impact collisions," *Annals of biomedical engineering*, vol. 49, p. 115–128, 2021.
- [48] I. Wochner, L. V. Nölle, O. V. Martynenko and S. Schmitt, "'Falling heads': investigating reflexive responses to head–neck perturbations," *BioMedical Engineering OnLine*, vol. 21, p. 25, 2022.
- [49] R. Happee, E. de Bruijn, P. A. Forbes, P. van Drunen, J. H. Van Dieën and F. C. T. Van Der Helm, "Neck postural stabilization, motion comfort, and impact simulation," in *DHM and Posturography*, Elsevier, 2019, p. 243–260.
- [50] R. D. Sacks and R. R. Roy, "Architecture of the hind limb muscles of cats: functional significance," *Journal of Morphology*, vol. 173, p. 185–195, 1982.
- [51] P. Netti, A. D'amore, D. Ronca, L. Ambrosio and L. Nicolais, "Structure-mechanical properties relationship of natural tendons and ligaments," *Journal of Materials Science: Materials in Medicine*, vol. 7, p. 525–530, 1996.
- [52] N. H. T. S. Administration, "Federal Motor Vehicle Safety Standards; Head Restraints," 2007.
- [53] A. Carlsson, Addressing female whiplash injury protection—a step towards 50th percentile female rear impact occupant models, Chalmers Tekniska Hogskola (Sweden), 2012.
- [54] J. Östh, M. Mendoza-Vazquez, A. Linder, M. Y. Svensson and K. Brodin, "The VIVA OpenHBM finite element 50th percentile female occupant model: whole body model development and kinematic validation," in *IRCOBI Conference*, 2017.
- [55] M. Millard, T. Uchida, A. Seth and S. L. Delp, "Flexing computational muscle: modeling and simulation of musculotendon dynamics," *Journal of biomechanical engineering*, vol. 135, 2013.
- [57] A. N. Vasavada, J. Danaraj and G. P. Siegmund, "Head and neck anthropometry, vertebral geometry and neck strength in height-matched men and women," *Journal of biomechanics*, vol. 41, p. 114–121, 2008.

182
183
184
185
186
187

188

APPENDIX A

189 Table 1: Architectural properties of the MAT_156 and the VEXAT cat soleus models used to simulate Herzog and Leonard
190 [9]. The values for ℓ_o^M and f_o^M differ in the direction of the CE to accommodate for the VEXAT's pennation model: the
191 values of ℓ_o^M and f_o^M are identical when evaluated along the VEXAT's tendon.

Parameter	Symbol	MAT_156	VEXAT	Source
Optimal CE Length	ℓ_o^M	42.5 mm	42.9 mm	[9]
Pennation Angle	α	0°	7°	[50]
Max. Isometric Force	f_o^M	21.6 N	21.8 N	[9]
Max. Shortening Vel.	v_{MAX}^M	4.5 ℓ_o^M /s	4.5 ℓ_o^M /s	[38]
Tendon Slack Length	ℓ_s^T	30.5 mm	30.5 mm	[39] [9]
Tendon Stiffness	k_o^T	(rigid)	30 f_o^M / ℓ_s^T	[39]
Norm. Tendon Damping	U	(rigid)	0.057 1/s	[51]
ECM Fraction	P	-	56%	[37]

192